

AD690947

THE UNIVERSITY OF TEXAS AT AUSTIN

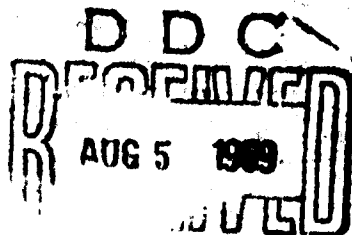
ARL-TR-69-17
August 1969

Copy No. 30

TURBULENT BOUNDARY LAYER SEPARATION AHEAD OF CYLINDRICAL PROTUBERANCES IN SUPERSONIC FLOW

J. H. Mashburn

NAVAL AIR SYSTEMS COMMAND
APL/JHU Subcontract 271734, Task B



ARL-TR-69-17
August 1969

**TURBULENT BOUNDARY LAYER SEPARATION
AHEAD OF CYLINDRICAL PROTUBERANCES IN SUPERSONIC FLOW**

J. H. Mashburn

This work has been sponsored by the Naval Air Systems Command
Under Subcontract 271734 with the Applied Physics Laboratory
of The Johns Hopkins University

This document has been approved
for public release and sale;
its distribution is unlimited.

**APPLIED RESEARCH LABORATORIES
THE UNIVERSITY OF TEXAS AT AUSTIN
AUSTIN, TEXAS 78712**

ABSTRACT

The results of an experimental study of separation distances ahead of right circular cylinders mounted perpendicular to a flat plate are presented. The tests were conducted in a supersonic wind tunnel at a nominal test Mach Number of 4.8. Turbulent boundary layer conditions existed at the cylinder mounting position. All tests were for single cylinder configurations. The cylinders tested ranged in length from 1/16 in. to 1 1/2 in. and in diameter from 3/16 in. to 1 1/2 in. Experimental data were used to determine an empirical correlation between boundary layer separation distance and cylinder length. Comparison of results with other data sources showed the correlation in close agreement with previously observed boundary layer separation phenomena.

PREFACE

The problem of the separation of a turbulent compressible boundary layer ahead of surface protuberances is a matter of considerable interest in the design of high-speed aerospace vehicles. Flow separation ahead of surface protuberances complicates the estimation of protuberance drag. One method of estimating drag in separated flow utilizes the boundary layer separation distance as a correlating parameter.

The current study, which correlates separation distance to protuberance length, is part of a general investigation into protuberance drag conducted by the Applied Research Laboratories (ARL) of the University of Texas at Austin. This study has been supported by the Applied Physics Laboratory of The Johns Hopkins University through APL/JHU Subcontract 181471, Task E and Subcontract 271734, Task B.

The author would like to express his appreciation to Dr. John C. Westkaemper, Research Engineer, for his guidance and cooperation and to the other members of the Aeromechanics Division for their considerable efforts in conducting the experimental work.

James Harvel Mashburn

Austin, Texas

August 1969

TABLE OF CONTENTS

	<u>Page</u>
ABSTRACT	iii
PREFACE	iv
NOMENCLATURE	vii
I. INTRODUCTION	1
II. APPARATUS	3
A. Wind Tunnel	3
B. Flat Plate	3
C. Cylinders	5
D. Instrumentation	6
III. TEST PROCEDURE AND DATA REDUCTION	7
IV. RESULTS AND DISCUSSION	9
A. Boundary Layer Thickness	9
B. Boundary Layer Separation	11
1. Short Cylinders	12
2. Intermediate Cylinders	12
3. Long Cylinders	13
V. ANALYSIS	14
A. Flat Plate Static Pressure Profiles	14
1. The Upstream Region	16
2. The Characteristic Separation Shock Wave	17
3. The Central Region	17
4. The Root Region	18
B. Separation Distance	19

TABLE OF CONTENTS (Cont'd)

	<u>Page</u>
VI. SUMMARY AND CONCLUSIONS	27
REFERENCES	29
TABLES	30
FIGURES	34

NOMENCLATURE

C_p	pressure coefficient $\frac{P - P_\infty}{q_\infty}$
D	cylinder diameter
f	ratio of momentum thickness to boundary layer thickness
h	height above flat plate test surface
K	stagnation condition constant
L	cylinder length
M	Mach Number
m	$M_\infty^2/5$
n	inverse of exponent in turbulent boundary layer assumed velocity profile
P	pressure
q	dynamic pressure
R_e	Reynolds Number
U	velocity
x	distance from plate leading edge
β	oblique shock wave angle
Δ	separation distance in diameters
δ	nominal boundary layer thickness

SUBSCRIPTS

P pressure measurement
x distance from plate leading edge
 ∞ free stream

I. INTRODUCTION

The nature of fluid flow around obstructions has long been a matter of concern in the field of fluid mechanics. The earliest efforts in this area were concerned primarily with incompressible, two-dimensional flows. Further studies through the years have expanded the scope by investigation of viscosity effects, three-dimensional flows, and supersonic flow conditions.

This concern about the nature of flow around protuberances has become increasingly important in the design of current aerospace vehicles. High-speed flight poses the problem of flow separation before surface protrusions, which can markedly effect the aerodynamic characteristics. Separation can, by altering the flow, produce shifts in aerodynamic loading. In addition, separation can cause localized areas of higher aerodynamic heating. This heating is a matter of definite concern for high-speed vehicle structures design.

Applied Research Laboratories of The University of Texas at Austin, through its Aeromechanics Division, has been conducting a multiphase study into the problem of drag due to surface protuberances in high-speed flow. Westkaemper (Ref. 1) has conducted an extensive study into the drag of such protuberances for a turbulent, supersonic boundary layer. Part of this study involved the determination of boundary layer separation distance as a function of cylinder size. Using this correlation, methods were deduced for calculating drag, the results of which compared favorably with measured values.

The purpose of the present study was to investigate further separation distances for various cylindrical protuberances. The complexity of the equations of viscous fluid motion, the Navier-Stokes equations, seems to preclude any analytical solution to the problem of flow separation at this time. Consequently, an empirical correlation for separation distance as a function of cylinder size was determined. Separation distances were determined by means of flat plate static pressure distributions. Results of the present study were compared with the results from previous data sources.

II. APPARATUS

A. Wind Tunnel

The tests were conducted in the ARL blowdown-type wind tunnel having test section dimensions of 6 in. x 7 in. and a nominal Mach Number of 5.0, provided by fixed nozzle blocks. The average Mach Number for the actual tests was 4.81. The tests were made under adiabatic flow conditions. Moisture condensation was prevented by the use of a stagnation temperature in the range from 137°F to 212°F. Moisture in the supply air was reduced by an aftercooler using water at room temperature. The supply air was compressed to 2500 psig before passing through the aftercooler. Heating of the supply air was accomplished by an integral electric heater located between the air storage tanks and the stilling chamber. Heating was automatically controlled to a preset value within $\pm 5^\circ\text{F}$ during each run. Stilling chamber pressure was also automatically controlled within ± 3 psi, with a range used during the tests of 254 to 263 psig.

B. Flat Plate

The tests were made using the flat plate shown in Fig. 1. The plate, constructed of $3/4$ in. thick aluminum, was 6 in. wide and 17.5 in. long. Having the plate width approximately equal the width of the wind tunnel allowed the plate to be mounted between the tunnel side walls. The plate test surface was positioned 0.19 in. below the horizontal plane of symmetry of the two-dimensional nozzle. The

leading edge of the plate had a wedge angle of 12.1 deg on the side opposite the plate test surface. A boundary layer tripper strip, consisting of a 1/2 in. wide strip of 80 grit emery cloth, was mounted on the test surface approximately 1/2 in. downstream of the leading edge. The cylinder test station was located 13.5 in. from the leading edge. The boundary layer thickness on the plate at that point was approximately 0.25 in.

Pressure data were obtained by means of 84 static pressure taps installed along the plate centerline, upstream of the cylinder test station. From 0.25 in. to 5.0 in. upstream of the test station, the taps were located 1/16 in. apart. From 5.0 in. to 9.0 in. upstream the taps were located 1/2 in. apart. The orifices themselves were No. 79 (0.0145 in. diam) holes drilled in the test surface of the flat plate. Small lengths of stainless steel tubing were inserted and sealed with epoxy into countersunk No. 64 (0.036 in. diam) holes for each tap within the cavity on the underside of the plate. Lengths of flexible plastic tubing then led from each tap to longer lengths of stainless steel tubing that passed through the side of the plate. Three separate bundles of these longer tubes were encased in metal sleeves or plugs that extended through the tunnel side wall when the model was installed in the tunnel. Larger plastic tubing was then connected between the taps and the mercury manometer board. The flat plate details are shown in Figs. 2 and 3.

Because the run times were too short to allow the plate to obtain the recovery temperature by aerodynamic heating, electric preheating of the plate was employed. This preheating was accomplished

by Nichrome heating wires imbedded in a groove in the main body of the plate. This groove, running approximately 0.5 in. inside the edges, was located in the plate surface opposite the test surface. The wires were first run through ceramic tubes that were then imbedded in the grooves using porcelain cement. A thermocouple was installed in the plate to monitor the plate temperature. Rubber gasket material, placed in grooves on each side of the model, ran the length of the plate to provide a seal between the plate and the tunnel side walls. This seal prevented any airflow around the sides of the plate from one surface to the other.

C. Cylinders

Table I presents the dimensions of each cylinder tested. The cylinders used ranged in length from 1/16 in. to 1 1/2 in. and in diameter from 3/16 in. to 1 1/2 in. The cylinders were made of stainless steel and had threaded shanks for attachment to the flat plate. The 3/16 in. diam and 1/4 in. diam cylinders had 3/16 in. diam threaded shanks. The larger cylinder had 1/4 in. diam shanks that required refitting of the mounting hole in the plate at the test station. Attachment consisted of simply screwing the cylinders down tight and flush to the test surface. Thin Teflon tape wrapped around the cylinder shanks prior to attachment helped provide a tighter fit in the test plate. A tight fit was important in preventing cylinder rotation as the shock moved down the tunnel.

D. Instrumentation

The primary data obtained from these tests were the plate static pressures at various stations upstream of the cylinders. These pressures were indicated by means of a multitube mercury manometer and, following stabilization, were photographically recorded during each run. The stilling chamber pressure was indicated by a bourdon-type pressure gauge. The resistance heater within the plate was powered through a transformer for plate heating to the required recovery temperature. This temperature was measured by the thermocouple imbedded in the plate. Another thermocouple located in the stilling chamber measured stagnation temperature. Both of these temperatures were recorded by means of a Honeywell-Brown strip chart recorder.

III. TEST PROCEDURE AND DATA REDUCTION

The initial step prior to each run was to turn on the resistance heater and allow the flat plate to attain recovery temperature. This temperature, a function of the stagnation temperature, was approximately 145°F. Once the desired plate temperature was attained, the tunnel was started. The manometer board readings indicated when the flow had stabilized. After allowing a few more seconds for slight mercury column oscillations to decay, the manometer readings were recorded by Polaroid camera photographs. The stilling chamber stagnation pressure was manually recorded from the pressure gauge and the tunnel was then shut down. The plate temperature and stilling chamber stagnation temperature were monitored continuously throughout the run and recorded by means of the strip chart recorder.

As mentioned previously, there was a total of 84 static pressure taps installed in the flat plate. The multitube manometer board contained 50 mercury columns, one of which was required to indicate the reference level. It was, therefore, not possible to monitor all of the stations during any one run. To obtain the most meaningful measurements, pressures were monitored every 1/2 in. over the entire range for all runs, and the remaining stations were divided into seven groups that could be utilized, dependent on the anticipated separation distance. The predicted separation distances for the

various cylinder configurations were determined by use of the empirical separation distance-cylinder size correlations of Ref. 1 and 2. In practice, three groups of pressure taps (a total of 30 taps) from the previously mentioned seven groups were utilized for each run. For any cylinder configuration the groups of taps to be read were selected to give a concentration of pressure readings surrounding the predicted separation distance. This concentration was in addition to the pressure taps, spaced $1/2$ in. apart over the entire range, which were read for every run. The utilization of the various groups of taps was controlled by seven guillotines, located between the flat plate and manometer, that could shut off any selected groups of pressure taps.

The data collected from each run consisted of the static pressure distribution on the flat plate, stagnation temperature and pressure, and atmospheric pressure. The static pressures at the three foremost tap stations were averaged to yield the free-stream static pressure. This free-stream static pressure and the stagnation pressure were used to compute the Mach Number for each run. The free-stream temperature was computed from the stagnation temperature and Mach Number. Knowing free-stream pressure, free-stream temperature, and Mach Number allowed calculation of the free-stream density, velocity, and dynamic pressure. The dynamic pressure was then used to convert the static pressure distributions into coefficient form.

IV. RESULTS AND DISCUSSION

Prior to any discussion of experimental results, several general remarks should be noted. The primary objective of this study was to attempt a closer correlation between boundary layer separation distance and cylinder size. Toward this end, the prime experimental data generated consisted of static pressure distributions along the flat plate upstream of the test cylinders. No pressure measurements were made on the cylinders themselves.

A. Boundary Layer Thickness

Because the boundary layer is of major importance to this study, it is necessary to consider the nature and thickness of the boundary layer at the cylinder test section. No surveys of the boundary layer were made in the present study. The assumption of turbulent flow was made, however, since the average Reynolds Number, based on the distance from the plate leading edge, was 14.5 million at the test station. In the experimental work described in Ref. 1, impact-pressure surveys were made in the same wind tunnel and under nearly identical flow conditions as the present study. The model tested was also nearly identical, having the same reference lengths and surface finish as the present test model. The velocity profiles from those surveys indicated a turbulent boundary layer. The boundary layer thickness obtained from these surveys was approximately 1/4 in. at the cylinder test station.

Several analytic methods were used to calculate the approximate boundary layer height at the test station. It should be emphasized that the methods employed indicate the turbulent boundary layer growth for a smooth flat plate. As such, they are not really valid for a flat plate with a boundary layer tripper strip, as was the case in the present study. The smooth plate boundary layer thicknesses were calculated as rough approximations to the actual test section boundary layer thickness of the current experiments.

One such method of calculating boundary layer thickness was that derived by Lucero in Ref. 2. The predicted boundary layer growth was obtained from the expression

$$\frac{\delta}{X} = \frac{1}{2} \left[\frac{(n+1)(n+2)}{n} + 0.544M_{\infty}^2 \right] (1 + 0.0128M_{\infty}^2)^{-0.67} \times \frac{0.494}{(\log_{10} R_{e_x})^{2.64}}, \quad (1)$$

where n is the inverse of the exponent in the turbulent boundary layer assumed velocity profile. For this study n was assumed to be 7. The use of the above expression gave a value of 0.168 in. for the value of boundary layer thickness at the cylinder test station. For a one-seventh velocity profile, the classic equation for the ratio of boundary layer thickness to flat plate distance is a function of the fifth root of the Reynolds Number. The use of this equation gave a result of 0.185 in. thickness at the test station.

One additional method employed was that presented by Tucker in Ref. 7. The resultant expression for the existing zero pressures gradient case is

$$\delta = \frac{1}{f} \frac{7K}{6} \left[\frac{(1+m^2)^2}{M_\infty \left(1 + \frac{m^2}{2}\right)^5} \right]^{1/7} \times X^{6/7}, \quad (2)$$

where $m = \frac{M_\infty^2}{5}$. The ratio of momentum thickness to boundary layer thickness, f , is equal to 0.0418, and the stagnation condition constant, K , is equal to 0.00158. The use of the above expression gave a value of 0.222 in. for the boundary layer thickness at the cylinder test station.

From the above discussion it is seen that the analytic methods give results for boundary layer thickness at the cylinder test station that are consistently less than the experimental value obtained in the work of Ref. 1. This finding is to be expected since the analytical methods approximated the boundary layer growth on a smooth flat plate, and the measured thickness of Ref. 1 was obtained on a plate having a tripper strip. As the test conditions and plate dimensions for the experimental work of Ref. 1 were nearly identical to those of the present study, the previously measured thickness of 0.25 in. was assumed to be the boundary layer thickness at the cylinder test station for the present tests.

B. Boundary Layer Separation

As mentioned earlier, the cylinders tested ranged from 1/16 in. to 1 1/2 in. in length and from 3/16 in. to 1 1/2 in. in

diameter. Boundary layer separation occurred for all but the smallest of the test cylinders. The separation characteristics for the larger cylinders fell into two distinct groups, dependent upon cylinder length-to-diameter ratio. Based upon these observations, the cylinders tested were classified into three nominal groups according to their effect on the boundary layer flow.

1. Short Cylinders

Of the cylinders tested, separation did not occur for any of the shortest lengths (1/16 in.) or the smallest diameters (3/16 in.). These results implied that the onset of boundary layer separation is a function of both cylinder length and diameter (i.e. frontal area). The cylinders that did not induce separation had either or both dimensions small enough that the boundary layer was able to flow over or around the protuberance with a small enough adverse pressure gradient that the flow did not separate from the plate surface. The group of cylinders for which no boundary layer separation was induced are defined in this study as "short" cylinders.

2. Intermediate Cylinders

The cylinders defined as the intermediate group represent the most general case. In this case the cylinders, due to their larger size, are able to exert a greater influence on the boundary layer flow upstream of the protuberance. The boundary layer is not able to flow around or over the cylinder without the formation of an adverse pressure gradient great enough that the boundary layer is separated from the plate. The intermediate length cylinders, for any

given diameter, were observed to induce boundary layer separation for which the upstream separation distance was a function of cylinder length.

Figure 9 presents the results of the separation distance-cylinder length correlation. Both terms were nondimensionalized by dividing by the cylinder diameter. From the figure it can be seen that the separation distance varies with the cylinder length, up to a length-to-diameter (L/D) ratio of approximately 3.5.

3. Long Cylinders

For cylinders of $L/D > 3.5$, increasing length does not have an appreciable effect on the boundary layer separation distance. This fact can be seen in Fig. 9, as the separation distance/ D remains essentially constant for $L/D > 3.5$. The "long" cylinders represent the upper limit case in which the cylinders protrude far enough into the free-stream flow that increased length has no effect on the conditions within the boundary layer.

For the cylinders tested, the transition between the intermediate to the long classification occurred at an approximate length-to-boundary layer thickness ratio of 3 or 4. The flow geometry for the various cylinder size classifications is presented in Figs. 4 and 5.

V. ANALYSIS

The primary purpose of this study was, through the use of flat plate pressure distributions, to attempt accurate determinations of boundary layer separation distances and corresponding correlations to protuberance size. The following is an analysis of the results of this study.

A. Flat Plate Static Pressure Profiles

Some typical results of the present experimental study are shown in Figs. 6a through c. These figures show typical static pressure profiles ahead of the previously designated short, intermediate, and long cylinders. The latter two cases again are representative cylindrical protuberances that induce boundary layer separation. From the figures it can be seen that, in general, the flat plate static pressure profiles corresponding to boundary layer separation exhibit three distinct characteristics corresponding to different flow regions. The three separation pressure profile characteristics are as follows:

1. An initial rise in pressure occurs immediately downstream of the oblique shock wave induced by the separation of the boundary layer.
2. Following the initial pressure rise, the pressure decreases. This drop in pressure, which may decrease to approximately half the peak value, occurs in the area between the separated shear layer and the bow shock ahead of the protuberance.
3. A rapid increase in pressure occurs just ahead of the bow shock

The above static pressure profile regions have been noted by various investigators (Halprin, Lucero, et. al.) as characteristic of the pressure distribution in boundary layer separated flows. From earlier investigations utilizing pressure data on the flat plate and cylinders, schlieren photographs, and oil flow studies, a flow model associated with separated flow ahead of cylinders has been defined. Figure 5, based on Ref. 3, presents the flow model associated with boundary layer separation ahead of cylindrical protuberances in a supersonic airstream. Three general flow regions are shown, corresponding to the previously mentioned static pressure profile regions. In brief, the upstream region, located immediately after the oblique separation shock consists primarily of circumferential flow around the protuberance. The central region is an area of radial flow in the area of the separated shear layer. The root region consists of compressed flow aft of the protuberance bow shock. The results of the present study support the following analysis of these flow regions.

In the flow of a viscous fluid over a surface, the fluid within the boundary layer is retarded from the inviscid flow (free-stream) velocity by the shear forces initiated by skin friction. The velocity within the boundary layer varies from zero at the surface to that of the free-stream value. An obstruction to the flow, such as the cylindrical protuberances of the present study, will cause an increase in pressure ahead of the obstruction. This pressure can be created either by passing through a bow shock or by compression ahead of the obstruction. The increase in pressure causes a pressure force directed counter to the boundary layer flow. This adverse pressure

gradient then serves to deplete the momentum of the boundary layer fluid. Because the momentum of the boundary layer fluid is least at the surface, the fluid nearest the wall can be brought to rest first. If the adverse pressure gradient is sufficiently large to cause the fluid near the wall to move upstream, then boundary layer separation can occur at the most upstream position of the reversed flow. This upstream distance of the separation point is determined by the pressure buildup ahead of the protuberance. This previously mentioned pressure increase and, therefore, the separation distance is a function of flow conditions and protuberance size.

1. The Upstream Region

The effect of the separated boundary layer is to present an apparent change in surface contour to the oncoming flow. This abrupt change, therefore, induces an oblique shock wave immediately upstream of the separated flow. Figure 7, reprinted from Ref. 1, presents schlieren photographs of the boundary layer separation effects ahead of typical short, intermediate, and long cylinders. The oblique shock wave and the separated shear layer can clearly be seen in the latter two photographs in which separation occurs. A flow diagram, as previously mentioned, is presented in Fig. 5. The initial rise in pressure for the flat plate static pressure profiles is brought about by the deceleration of the upstream flow passing through the oblique separation shock. The flow is slowed with a corresponding pressure recovery. The oblique shock wave front is curved, due to the three-dimensional shape of the protuberance. The effect of the curved shock-wave front is to cause the flow to turn outward. This change in the

direction of motion causes a further increase in pressure. Thus, the initial pressure rise of the upstream region is a combination of pressure increases brought about by passage through the oblique separation shock and circumferential flow around the cylindrical protuberance.

2. The Characteristic Separation Shock Wave

From the schlieren photographs of Fig. 7 and the flow model of Fig. 5, the interaction of shock waves for separated flow ahead of protuberances can be seen. The oblique shock wave induced by separation intersects, for sufficiently long cylinders, the standing bow wave ahead of the protuberance. The point of intersection is termed the triple point. Below this triple point, due to the reduced velocity behind the oblique shock, the bow wave is deflected toward the cylinder. The combination of the oblique shock and the two parts of the bow wave is known as a lambda shock, due to the similarity of its shape with the Greek letter (λ). Previous investigators have noted this lambda shock to be characteristic of boundary layer separated flow. The region behind the deflected bow wave is considered the root region, and the central region is that between the two "feet" of the lambda.

3. The Central Region

The pressure profile within the central region is characterized by a distinct drop in static pressure from the peak value obtained in the pressure buildup of the upstream region. The flow of this central region consists of radial flow outwards from the protuberance. Lange in Ref. 5 has shown that a region of circulatory flow exists in the region between the flat plate and the separated

shear layer. For two-dimensional protuberances the circulatory flow moves upstream from the protuberance root along the flat plate surface. The flow turns at the flat plate-shear layer intersection and moves back downstream along the lower surface of the shear layer, then back down to the test surface upstream of the protuberance bow shock, to complete the circulation. This circulation beneath the separated shear layer is partially responsible for the dip in static pressure within this central region. For three-dimensional protuberances, such as the cylinders of the present study, the flow along the plate is radial with respect to the cylinders. This divergent flow for three-dimensional protuberances was found by Lange to produce greater static pressure dips than those encountered for corresponding two-dimensional obstructions. Thus, the dip in pressure within the central region is a combination of radial flow away from the protuberance and circulation of the flow beneath the separated shear layer.

4. The Root Region

The third pressure profile characteristic noted for separated flow was a rapid increase in static pressure between the bow shock and the protuberance root. This pressure increase is primarily due to the compression of the flow in passing through the protuberance bow shock. Sykes (Ref. 6) found that the presence of a blunt body in a shear layer causes the streamlines in the fluid approaching the body to bend towards the region of low pressures. Previous investigations considering the pressure distribution on the protuberance itself have shown that, in general, the pressure increases in the root region with vertical height up to the approximate height of the triple point.

This increase is shown in Fig. 8. Thus, an additional rise in pressure upon nearing the cylinder root is realized by the fluid from near the lower edge of the separated boundary layer being turned toward and brought to rest at the root. The sudden increase in pressure within the root region is, therefore, explained by the compression of the flow passing through the bow wave and being brought to rest near the cylinder root.

B. Separation Distance

Before beginning the present study, a preliminary literature search was conducted to determine the extent and scope of investigations into step-induced boundary layer separation. It was found that the bulk of the investigations dealt with two-dimensional protuberances, such as steps or ramps. Of those studies dealing with three-dimensional protuberances, the works of Westkaemper (Ref. 1) and Lucero (Ref. 2) contained considerable information concerning boundary layer separation distances ahead of cylinders. The study of Ref. 1 was conducted at the same Mach Number as the present study, while that of Ref. 2 was conducted at a lower Mach Number. The results of both studies will be discussed in greater detail.

As mentioned earlier, the separation distance was determined by means of flat plate static pressure profiles. The separation point was defined as the point of the initial pressure rise. The separation distance was measured in the stream direction from the cylinder stagnation line. For the present tests, the Mach Number, Reynolds Number, and boundary layer conditions were essentially constant. Thus, these

quantities could not be considered variables in any empirical correlation of separation data.

The parameters that were valid variables for separation data correlation in this study were the cylinder length and diameter, and the cylinder size was the only variable between experimental runs. The method selected for correlating the results was to use the cylinder diameter to nondimensionalize both the separation distance and the cylinder length, as shown in Fig. 9. The results of this study were expressed empirically by the use of an nth order curve fit computer program. The curve drawn through the data points in Fig. 9 is a fifth order least squares curve fit. The fifth order curve gave the least residuals of the curve fits that were attempted. The empirical separation distance-cylinder size correlation, as expressed by the previous equation, is as follows:

$$\begin{aligned} \Delta = & 0.009 (L/D)^5 - 0.163 (L/D)^4 + 1.061 (L/D)^3 \\ & - 3.210 (L/D)^2 + 4.710 (L/D) - 0.009 \quad , \end{aligned} \quad (3)$$

where Δ = separation distance/diameter.

From Fig. 9 it can be seen that the plotted curve tends to oscillate for the higher L/D ratios. This oscillation is due to the inflections inherent in an nth order polynomial equation. A higher order curve fit would exhibit a greater number of, but less pronounced, inflections. Increasingly higher order curve fits would approach a true asymptotic curve, as expected from physical reasoning.

In considering the experimental measurements and correlation of results, some discussion of accuracy is in order. The separation point is defined as the initial rise in static pressure. The measured separation distance is the distance from the cylinder leading edge upstream to the centerline of the pressure tap registering the initial pressure rise. The actual separation point, however, could lie anywhere between the two pressure taps that bracket the tap registering the initial pressure rise. The maximum uncertainty of the separation distance measurement is equal to the spacing between consecutive pressure taps (1/16 in. for the present study). For the empirical correlation of Fig. 9, the uncertainty of the data points is equal to the uncertainty of the separation distance measurements divided by the diameter, or $1/16/D$. Thus it can be seen that the accuracy of the data points in Fig. 9 is a function of cylinder diameter. As the cylinder diameter becomes smaller, the uncertainty of the measurement increases. Therefore, in general, the accuracy of the data points in Fig. 9 decreases as the cylinder L/D ratio increases. This decrease is due to the fact that the higher L/D ratios were obtained by using successively smaller diameter cylinders. Considering the uncertainty of the data points as a function of the cylinder diameter, a better separation distance-cylinder size correlation could be obtained by means of a weighted curve fit, based on cylinder diameter.

From the results of previous investigations it has been shown that, for a sufficiently long cylinder, any increase above that length seems to have no effect on the separation distance. Thus, it is natural to assume that there is some upper limit for which an increase in L/D has no effect on Δ . This assumption is shown in Fig. 9, since for

L/D greater than 3.5, the empirical curve tends to become approximately horizontal, indicating a constant separation distance of about 3.1 diam. Corresponding to this, Westkaemper reported in Ref. 1 that for L/D greater than 1.13, the separation distance is 2.65 diam.

A lower limit for the separation correlation must also exist, since it was found that separation did not occur for the smallest lengths or diameters. Table I summarizes the configurations tested and whether separation occurred. The criteria used for determining boundary layer separation have been discussed previously. The pressure distributions for separated flow exhibit an initial rise in pressure followed by a pressure drop to approximately half the peak value, with a second increase in pressure occurring just upstream of the cylinder. For flows that did not have these three characteristics, it was assumed that boundary layer separation had not occurred. Most of the unseparated cases had pressure distributions that exhibited only the initial pressure rise. For these cases the protuberances, while large enough to decelerate the flow with an accompanying pressure rise, were not sufficiently large to cause boundary layer separation. Several of the cylinders tested produced pressure distributions, satisfying the first two criteria, that would tend to indicate that boundary layer separation had occurred. The pressure drop following the initial rise was very slight however. Since earlier flat plate tests (no protuberance) had indicated that the particular taps recording this slight pressure dip tended to read lower than average values, the validity of the pressure drop was questioned. For cases satisfying the first two criteria, it was assumed that boundary layer separation did not occur. Boundary

layer separation occurred in this study for a minimum L/D of 0.083. This separation distance was for a cylinder having a length of 0.125 in. and a diameter of 1.5 in. Based on the assumed boundary layer thickness of 0.25 in. at the test station, this minimum case corresponded to an L/δ ratio of approximately 0.5. This value can be compared with the results of Ref. 2, where it was noted that the characteristic separation pressure profiles were not observed for $L/\delta \leq 0.6$. Thus, it can be stated that the empirical separation distance expression in this study has not been shown valid for $L/D < 0.83$ or for cylinder lengths less than 0.5 times the boundary layer thickness.

Several sources of data were used to evaluate the results of the present study. One of these was the previously mentioned work of Ref. 1. These tests were conducted at an average Mach Number of 4.91 and at a measured boundary layer thickness of approximately $1/4$ in. The free-stream Reynolds Number was 0.96 million per inch. The separation distance was determined by means of oil flow measurements. The forward boundary of the oil flow pattern was assumed to be the initial separation point. The data points from this source, which are presented in Fig. 9, are representative values that most nearly approximated the empirical correlation of that study. It can be noted from Fig. 9 that the results of Ref. 1 are in good agreement with the present tests, up to an L/D of about 2.0. For larger values of L/D the results of Ref. 1 show, as previously noted, a near constant separation distance of approximately 0.4 diam less than the present study.

It is felt that the variation in the results of the two studies is due primarily to the two methods of determining the separation distance. In Ref. 8 it was noted that the pressure difference across the oblique shock wave must spread out in a fan-like manner in the boundary layer near the wall. This is illustrated in Fig. 10. The diffusion of the shock-wave pressure, both to the front and rear of the nominal shock position, is believed the primary cause of the difference in results between Ref. 1 and the present study. In the present study the separation point was defined as the point of the initial pressure rise. This rise would occur at the most forward point of the diffused shock near the wall. For the oil flow studies, however, the separation point was considered the forward point of the oil flow. In the tests of Ref. 1 the oil mixture was released into the flow between the cylinder and the anticipated separation station. The radial flow in the central separated region carried the oil to its most upstream position. This position was determined by a balance of pressure between the flow regions. The oil mixture was able to move upstream until the static and dynamic pressures of the radial flow region were balanced by the static and dynamic pressures upstream. The separation shock retards the oil mixture, as the oil flowing upstream encounters the strong adverse pressure gradient produced by the shock wave. The most forward position of the oil flow would, therefore, likely be near the downstream region of the diffused shock near the wall. Thus, the separation distances obtained by these two methods would vary due primarily to the shock wave diffusion region. With increasing separation distances and, therefore, increasing L/D ratios,

the oblique shock angle, β , decreases. As the shock-wave angle becomes more oblique, it would seem that this fan-like region would tend to diffuse proportionally more in the upstream direction, which might explain the larger values obtained in the present tests for the larger L/D ratios. This explanation is a matter of conjecture, however, lacking additional information on the oblique shock-wave diffusion process in the boundary layer.

A second source of data for the evaluation of the present results was the previously mentioned work of Ref. 2. These tests were conducted at a Mach Number of 2.17 and a Reynolds Number, based on the distance from the plate leading edge, of 2.4 million. The calculated boundary layer thickness was 0.17 in. Tests were conducted on cylinders of 0.6 in. diam and 1.0 in. diam, with lengths of from 0.05 in. to 0.75 in. The separation distance was determined by static pressure measurements on the flat plate ahead of the cylinder, as in the present study. Results from Ref. 2 are also shown in Fig. 9. They are in substantial agreement with the results of the present study for the entire range of tests for Ref. 2. No tests were conducted in that study for the higher values of L/D.

One additional data point was obtained from the tests of Ref. 3. Tests were conducted on a 1.0 in. diam, 0.25 in. long cylinder at a Mach Number of 2.71. The boundary layer thickness of 0.17 in. and the Reynolds Number were unspecified. This data point, shown in Fig. 9, agreed very well with the correlation of Eq. (3).

Data points for nominally infinite length cylinders (extending completely across the flow) were obtained from Ref. 9.

The tests were conducted at a Mach Number of 2.5 and a Reynolds Number (based on flat plate length to cylinder station) of 18.5 million. The values of separation distance obtained varied from approximately 2.1 to 2.7 diam with the protuberances varying from 30 mm to 6 mm respectively. These tests indicated variable asymptotes on nondimensionalized separation distance, dependent on the protuberance diameter.

From the data presented in Fig. 9 for the present tests and the other sources, it can be seen that Eq. (3) provides a reasonably good correlation for separation distances ahead of cylindrical protuberances over a range of supersonic flow conditions. Although some slight deviation from previous results was noted for the higher L/D ratios, it is felt that the static pressure measurements would tend to be more accurate than the oil flow measurements, due primarily to the number and close spacing of the pressure taps employed in this study. The overall validity of the results of this study appear to be substantiated by close agreement with the results of the other data sources.

VI. SUMMARY AND CONCLUSIONS

Measurements were made of boundary layer separation distances ahead of right circular cylinders mounted on a flat plate for Mach 4.61 flow. A turbulent boundary layer existed and was approximately 0.25 in. thick at the test station. The corresponding length Reynolds Number was approximately 14.5 million. The cylinders tested ranged in length from 1/16 in. to 1 1/2 in. and in diameter from 3/16 in. to 1 1/2 in. The boundary layer separation distances were determined by means of static pressure measurements on the flat plate upstream of the cylindrical protuberances. These static pressure measurements were used to obtain an empirical correlation of boundary layer separation distance as a function of cylinder length and diameter.

The analysis of tests conducted in this study led to the following conclusions and recommendations.

1. The separation distance-cylinder size correlation obtained in this study was found to show close agreement with measured values over a wide range of cylinder configurations. Comparison of the results of this study with other data sources showed the correlation to be in close agreement with other tests. This agreement was encouraging because the other tests were made at Mach Numbers of 2.17, 2.71, and 4.9. Differing Reynolds Numbers for the other tests also tend to indicate the applicability of the present correlation over the previous range of supersonic flow.

2. A lower limit on cylinder size exists for which boundary layer separation is no longer induced. The minimum cylinder diameter

tested, regardless of length, for which separation occurred was 1/4 in. For diameters smaller than this limit, the boundary layer could presumably flow around the obstruction without sufficient perturbations to induce separation. Conversely, the minimum length, regardless of diameter, necessary to induce separation was 1/8 in.

3. A correlation of minimum cylinder size necessary to induce boundary layer separation vs boundary layer height would give greater insight into the prediction of protuberance-induced separation. This problem is proposed as a possible area of future study.

REFERENCES

1. Westkaemper, J. C., "The Drag of Cylinders All or Partially Immersed in a Turbulent, Supersonic Boundary Layer," Report No. DRL-549, Defense Research Laboratory, The University of Texas, Austin, Texas, March 1967.
2. Lucero, E. F., "Turbulent Boundary Layer Separation Induced by Three-Dimensional Protuberances on a Flat Plate," MS Thesis, University of Maryland, June 1966.
3. Halprin, R. W., "Step Induced Boundary-Layer Separation Phenomena," AIAA J. 13, No. 2, (1965), p. 357.
4. Gillette, W. B., "Separation Measurements of Supersonic Turbulent Boundary Layers Over Compression Corners," Report No. DRL-543, Defense Research Laboratory, The University of Texas, Austin, Texas, July 1966.
5. Lange, Roy H., "Present Status of Information Relative to the Prediction of Shock-Induced Boundary-Layer Separation," NACA TN 3065, February 1954.
6. Sykes, D. M., "The Supersonic and Low-Speed Flows Past Circular Cylinders of Finite Length Supported at One End," J. Fluid Mech. 12, (1962), pp. 367-387.
7. Tucker, Maurice, "Approximate Calculation of Turbulent Boundary-Layer Development in Compressible Flow," NACA TN 2337, 1951.
8. Donaldson, C. duP., and R. H. Lange, "Study of the Pressure Rise Across Shock Waves Required to Separate Laminar and Turbulent Boundary Layers," NACA TN 2770, September 1952.
9. Voitenko, D. M., A. I. Zubkov, and Yu. A. Panov, "Supersonic Gas Flow Past a Cylindrical Protuberance on a Plate," Akad. Nauk SSSR, Izv., Mekhan. Zhidkosti i Gaza, No. 1, (1966), pp. 121-125, (Applied Physics Laboratory/The Johns Hopkins University Translation TG 230-T 515).
10. Schlichting, H., Boundary Layer Theory, McGraw-Hill Book Company, 4th Edition, 1960.
11. Ames Research Staff, "Equations, Tables and Charts for Compressible Flow," NACA TR 1135, 1953.

TABLE I. CYLINDER CONFIGURATIONS TESTED
CYLINDER DIMENSIONS
(in inches)

<u>Diameter</u>	<u>Length</u>									
	1/16	1/8	1/4	3/8	7/16	1/2	3/4	1	1 1/4	1 1/2
.1875	NS	NS	NS	NS		NS	NS	NS	NS	NS
.250	NS	NS	NS	NS		NS	S	S	S	S
.300	NS	NS	S			S		S		S
.450	NS	S	S	S		S		S		S
.600		S	S	S	S	S		S		S
.750	NS	S	S	S		S		S		S
1.00	NS	S	S	S		S		S		S
1.25	NS	S	S	S		S		S		S
1.50	NS	S	S	S		S		S		S

S - Separation occurred

NS - No separation

blank - No test

TABLE II. EXPERIMENTAL DATA

<u>Run No.</u> (valid tests only)	<u>Length</u> (inches)	<u>Diameter</u> (inches)	$\Delta \left[\frac{\text{separation dist.}}{\text{diameter}} \right]$ (where applicable)
16	1.25	0.1875	
17	1.25	0.1875	
18	0.75	0.1875	
19	0.75	0.1875	
20	0.375	0.1875	
21	0.375	0.1875	
22	0.5	0.1875	
23	0.5	0.1875	
24	0.25	0.1875	
25	0.25	0.1875	
27	0.125	0.1875	
29	0.0625	0.1875	
30	0.0625	0.1875	
34	0.0625	0.25	
35	0.0625	0.25	
38	0.125	0.25	
39	0.25	0.25	
41	0.25	0.25	
43	0.375	0.25	
44	0.375	0.25	
45	0.5	0.25	
46	0.5	0.25	
47	0.75	0.25	
48	0.75	0.25	3.0
49	1.0	0.25	3.0
50	1.0	0.25	3.252
51	1.25	0.25	3.252
52	1.5	0.25	3.0
55	1.5	0.25	3.252
56	1.0	0.1875	
57	1.0	0.1875	

TABLE II. EXPERIMENTAL DATA (Cont'd)

<u>Run No.</u> (valid tests only)	<u>Length</u> (inches)	<u>Diameter</u> (inches)	Δ $\left[\frac{\text{separation dist.}}{\text{diameter}} \right]$ (where applicable)
58	1.5	0.1875	
59	1.5	0.1875	
89	0.125	0.3	
93	0.0625	0.3	
94	0.25	0.3	2.207
96	0.5	0.3	2.833
98	1.5	0.3	3.043
99	0.0625	0.45	
100	0.125	0.45	1.027
101	0.25	0.45	1.86
102	0.375	0.45	2.555
103	0.5	0.45	2.555
104	1.0	0.45	2.833
105	1.5	0.45	2.971
106	0.125	0.6	0.853
107	0.25	0.6	1.375
108	0.375	0.6	1.897
109	0.4375	0.6	2.105
111	0.5	0.6	2.208
112	1.0	0.6	2.625
113	1.5	0.6	2.833
114	0.0625	0.75	
115	0.125	0.75	0.667
116	0.25	0.75	1.084
117	0.375	0.75	1.667
118	0.5	0.75	2.084
119	0.375	1.0	1.375
120	0.5	1.0	1.688
121	0.375	1.25	1.15
122	0.0625	1.5	
123	0.125	1.5	0.375

TABLE II. EXPERIMENTAL DATA (Cont'd)

<u>Run No.</u> (valid tests only)	<u>Length</u> (inches)	<u>Diameter</u> (inches)	Δ $\left[\frac{\text{separation dist.}}{\text{diameter}} \right]$ (where applicable)
124	0.25	1.5	0.708
125	1.0	0.75	2.584
126	1.5	0.75	2.75
127	0.5	1.25	1.45
128	0.375	1.5	1.0
129	0.5	1.5	1.292
130	0.0625	1.0	
131	0.125	1.0	0.5
132	0.25	1.0	1.0
133	0.0625	1.25	
134	0.125	1.25	0.45
135	0.25	1.25	0.8
136	1.0	1.0	2.313
137	1.5	1.0	2.563
138	1.0	1.25	2.15
139	1.0	1.5	1.958
140	1.5	1.25	2.4
141	1.5	1.5	2.292
142	0.375	1.0	1.438

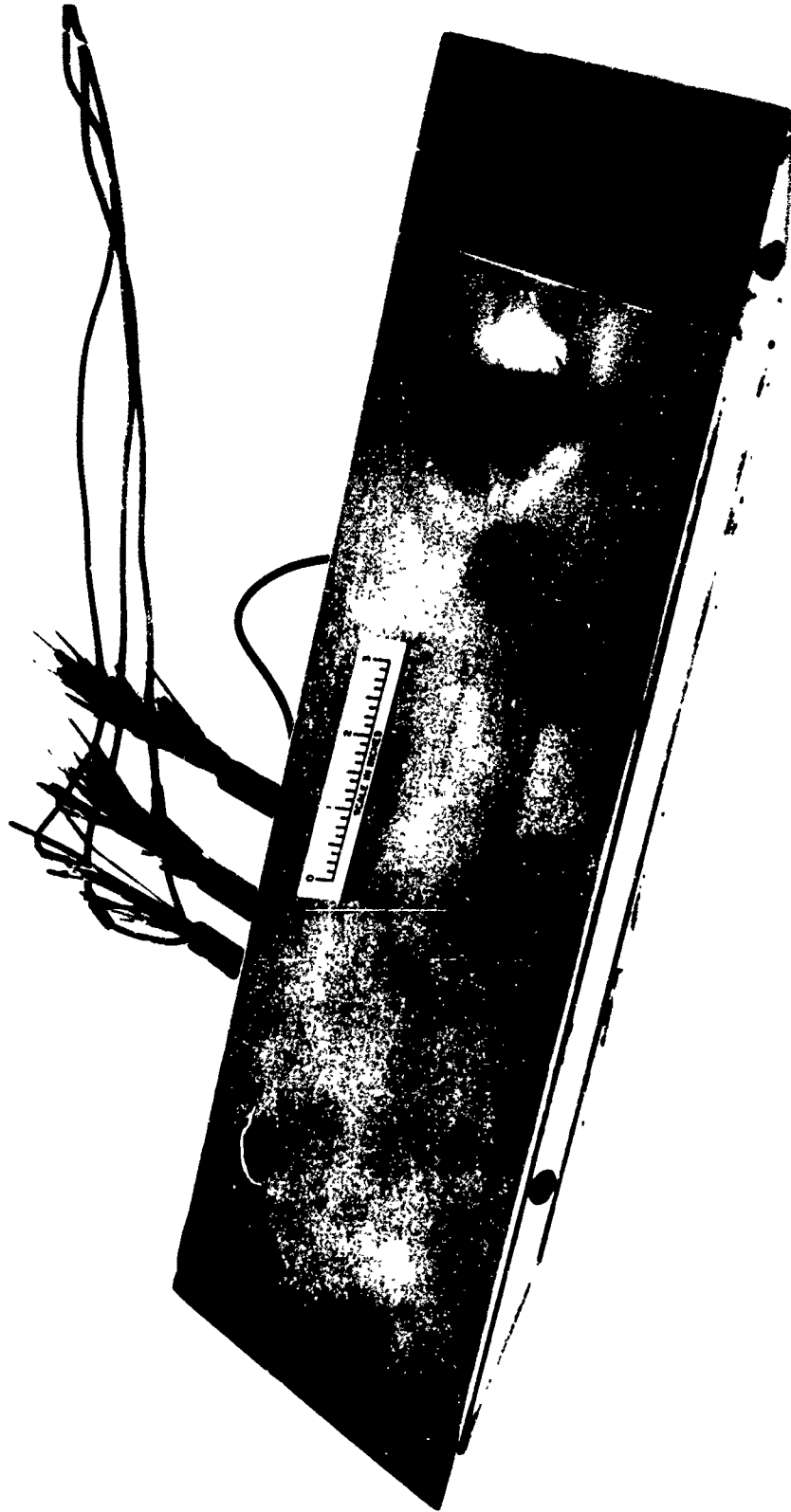


FIGURE 1
TEST PLATE AND CYLINDER FOR
SEPARATION DISTANCE DETERMINATION

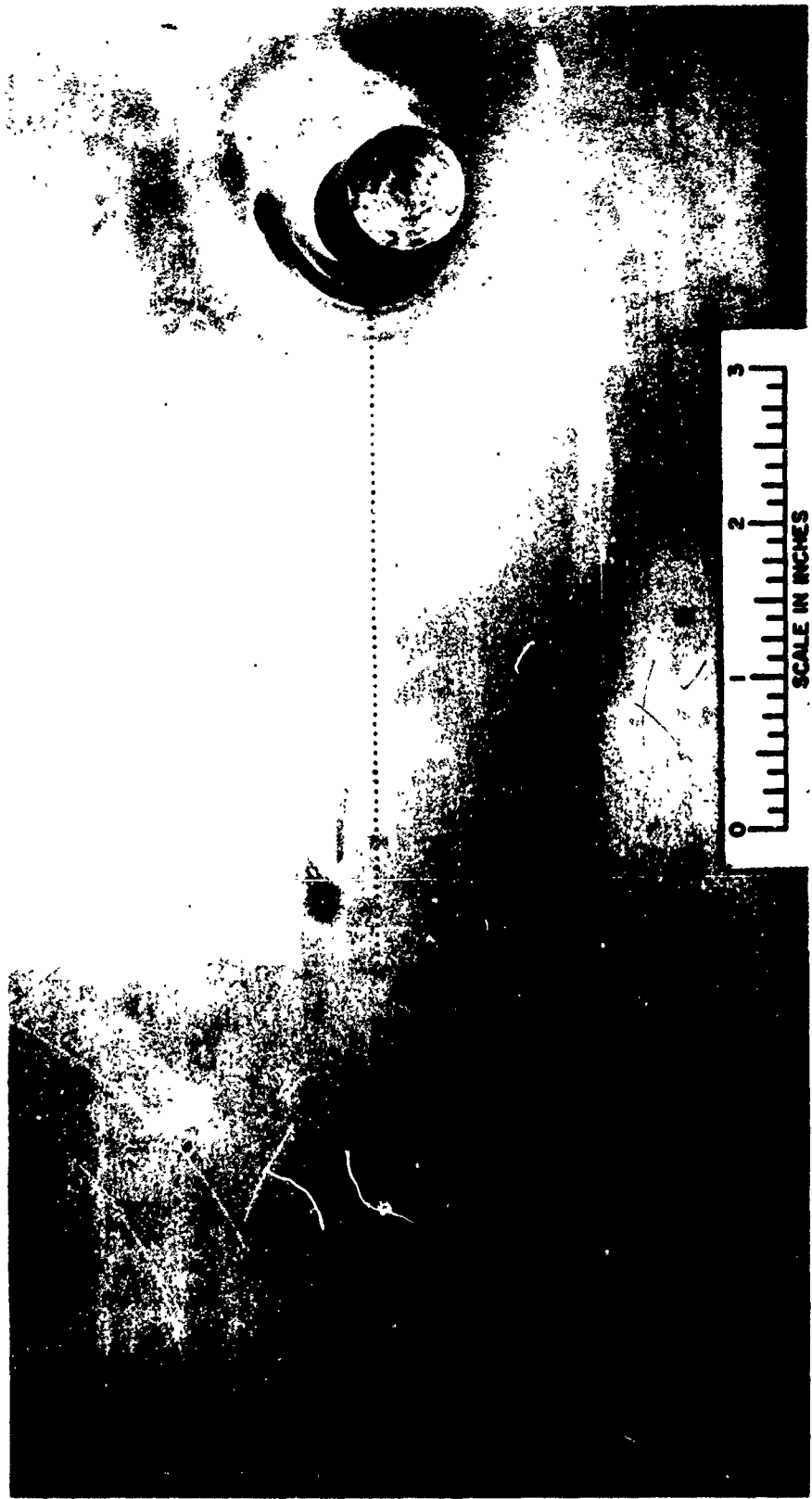


FIGURE 2
FLAT PLATE DETAIL SHOWING PRESSURE TAPS AND TYPICAL PROTUBERANCE

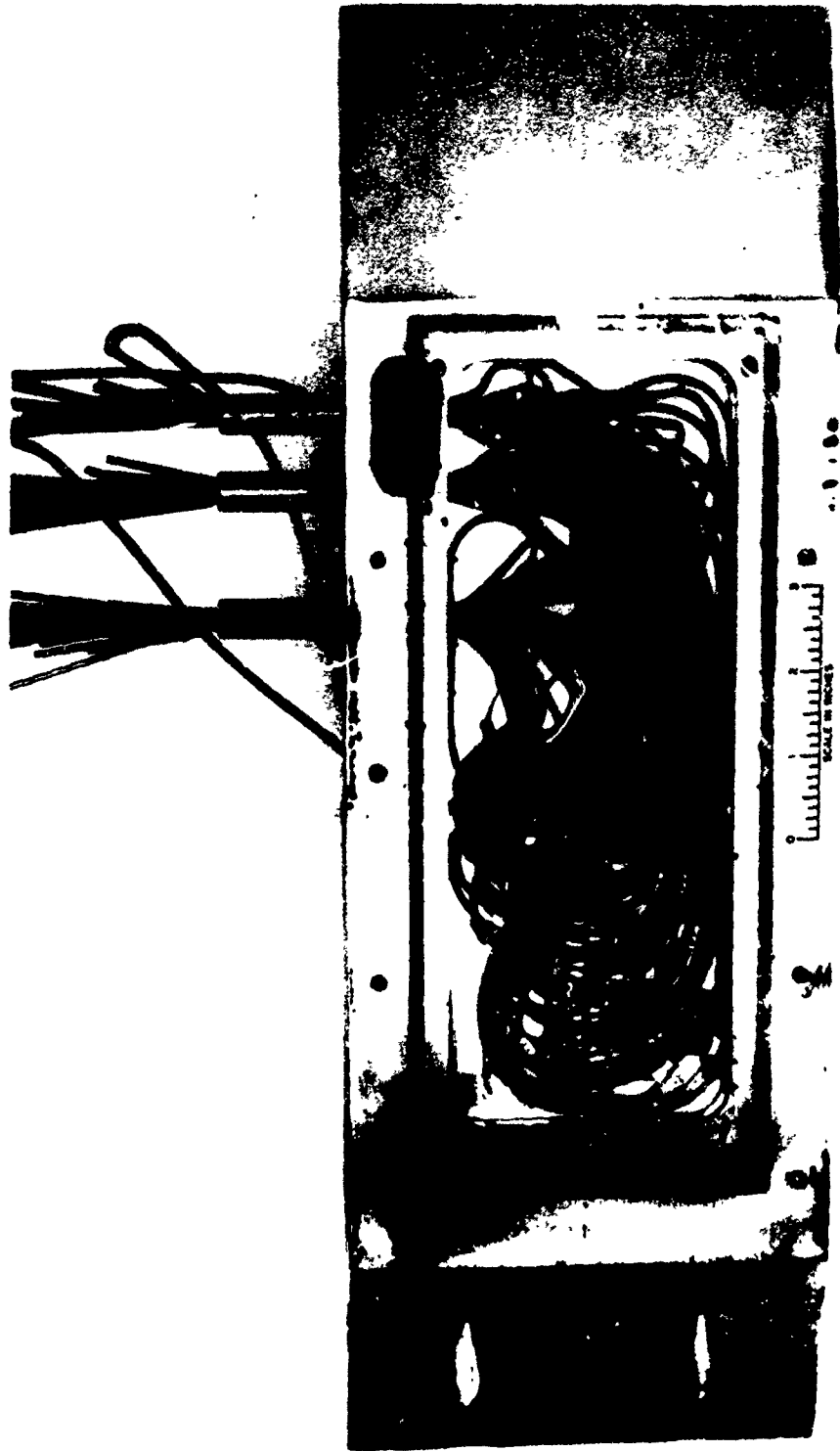


FIGURE 3
FLAT PLATE INTERIOR (COVER PLATE REMOVED)

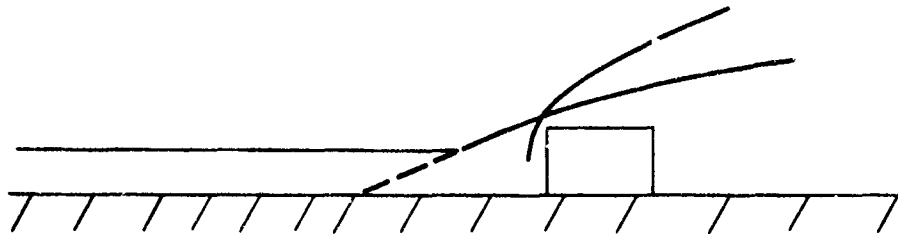
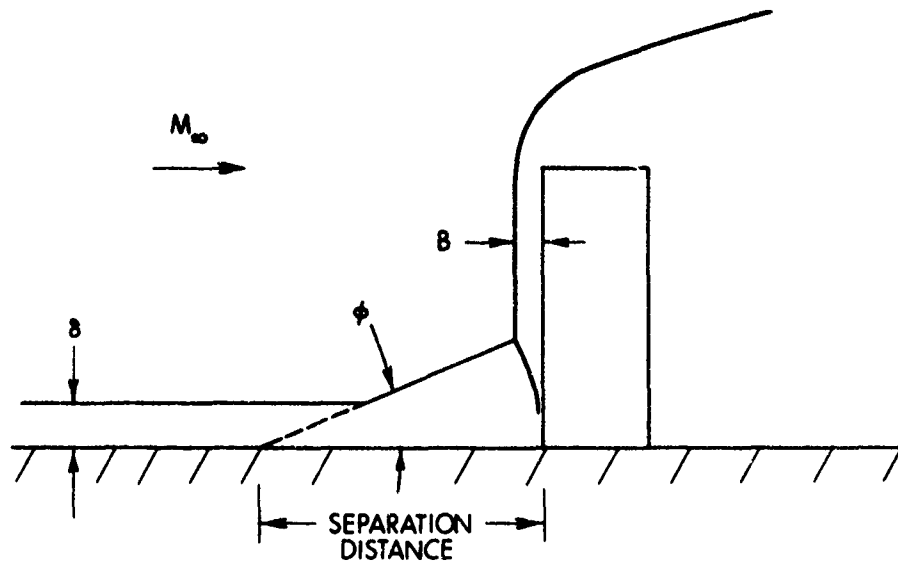


FIGURE 4
FLOW PATTERN DIAGRAMS
FROM REF. 1

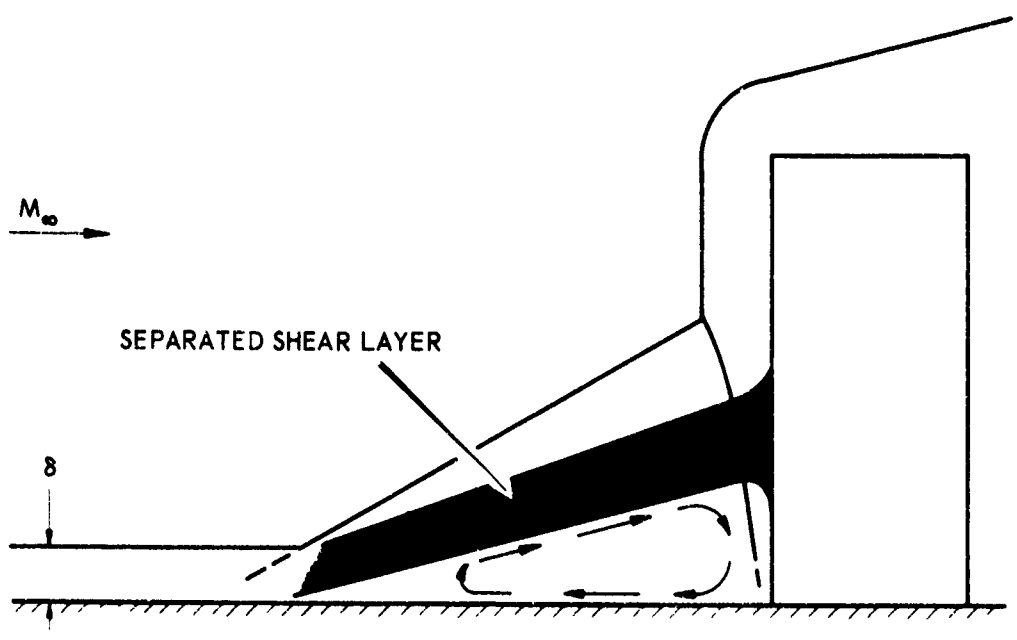
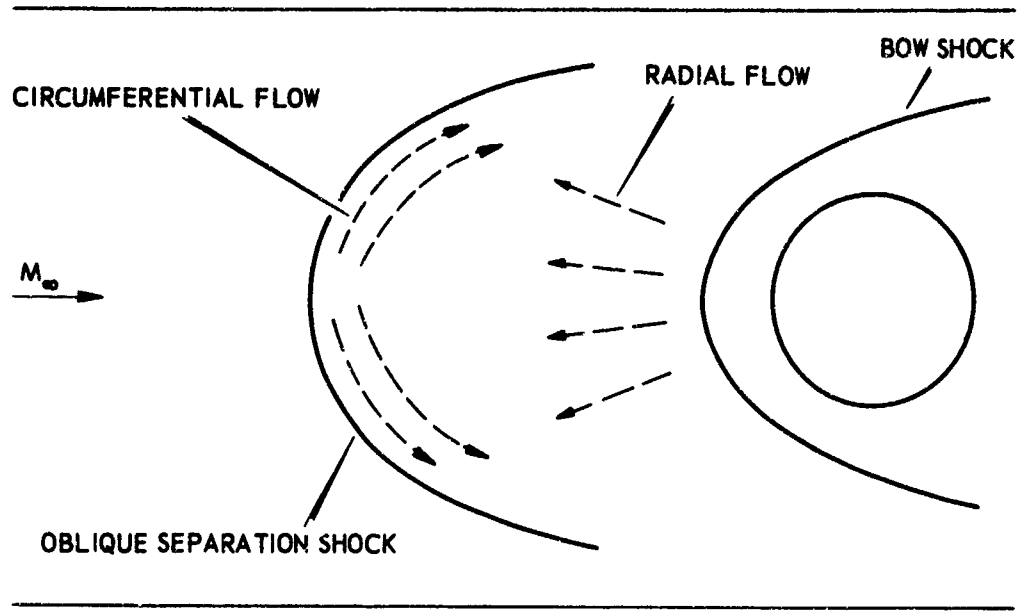


FIGURE 5
DETAILED BOUNDRY LAYER SEPARATION FLOW MODEL

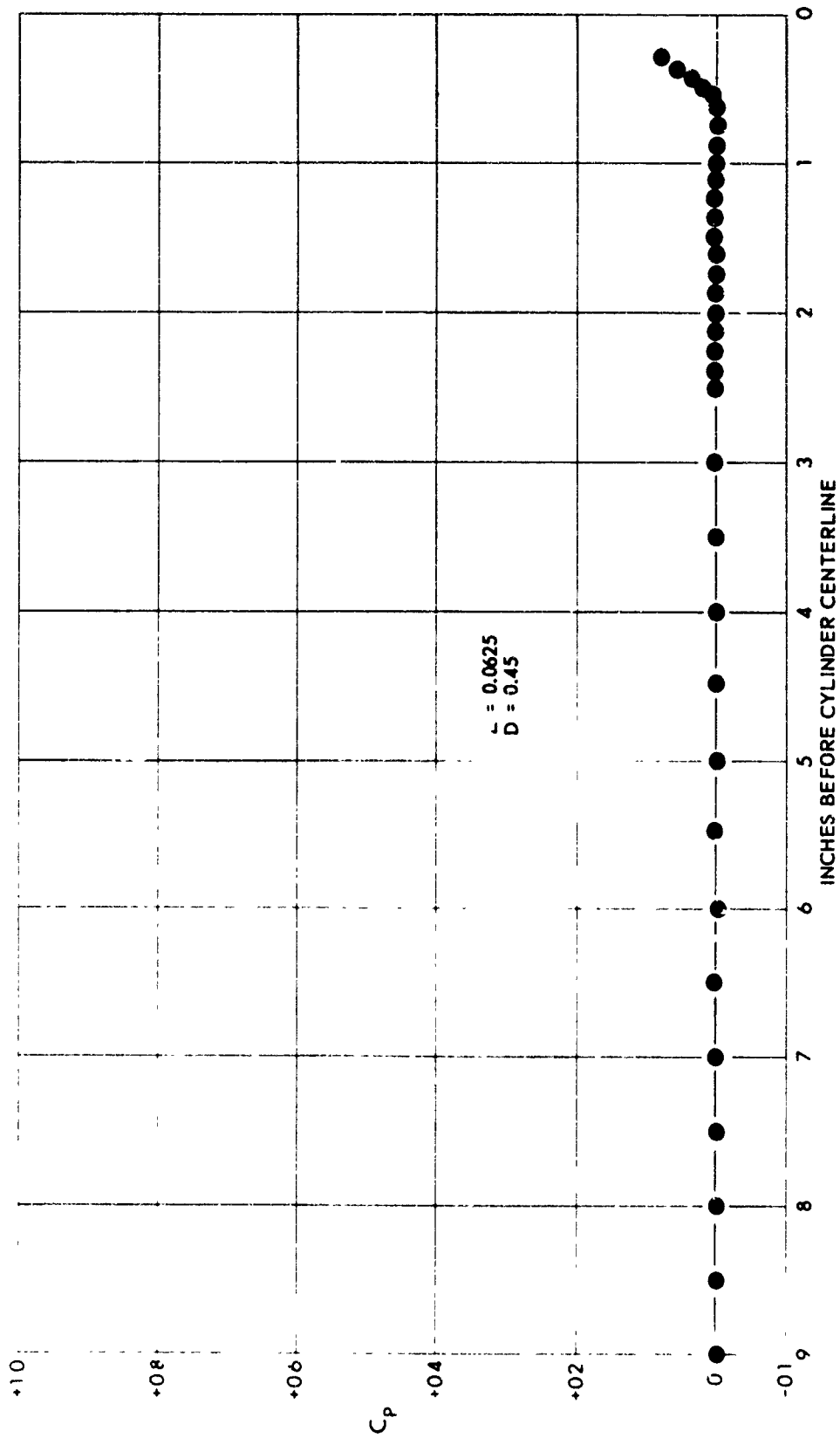


FIGURE 6a
TYPICAL STATIC PRESSURE PROFILE

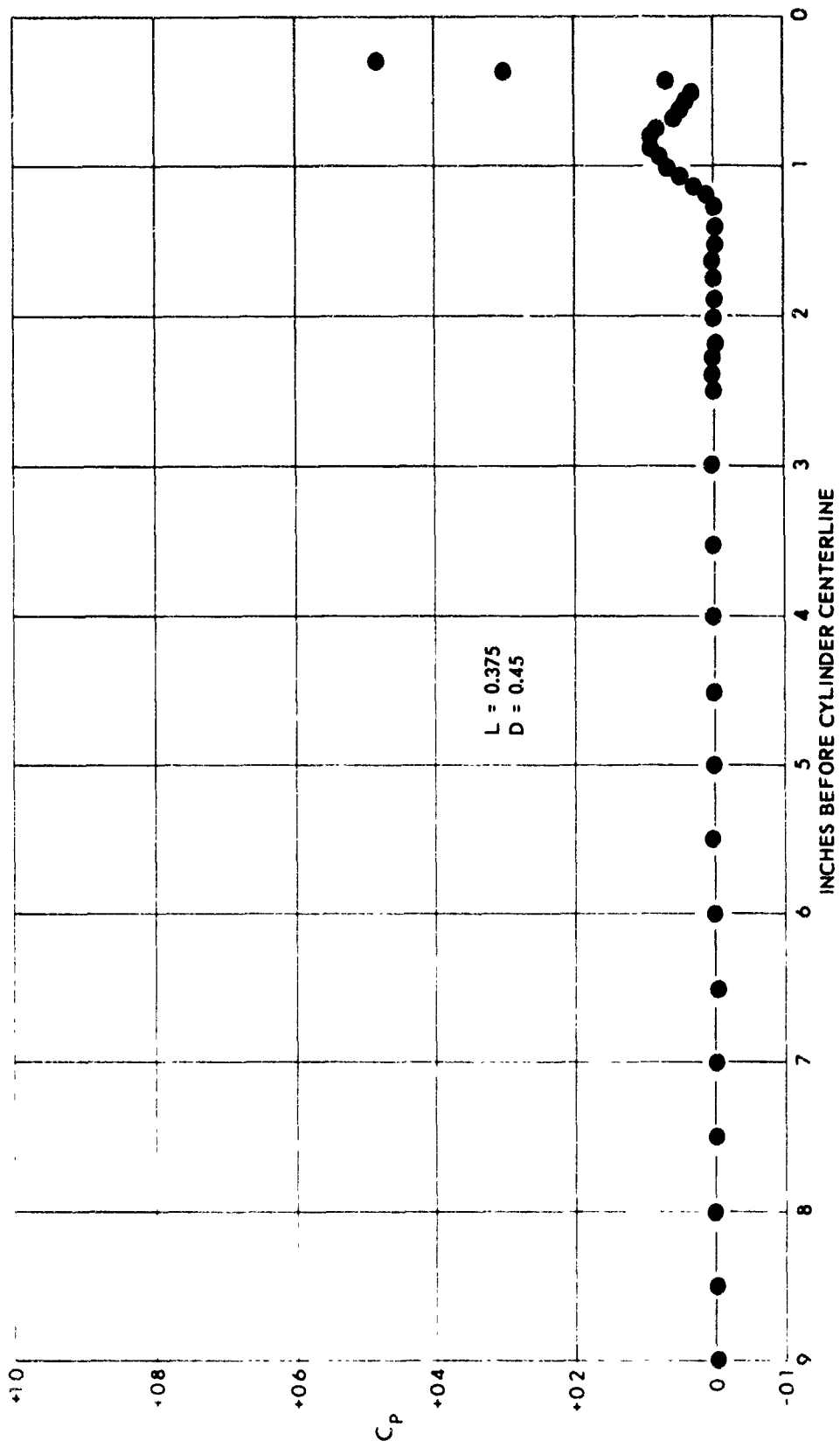


FIGURE 6b
 TYPICAL STATIC PRESSURE PROFILE

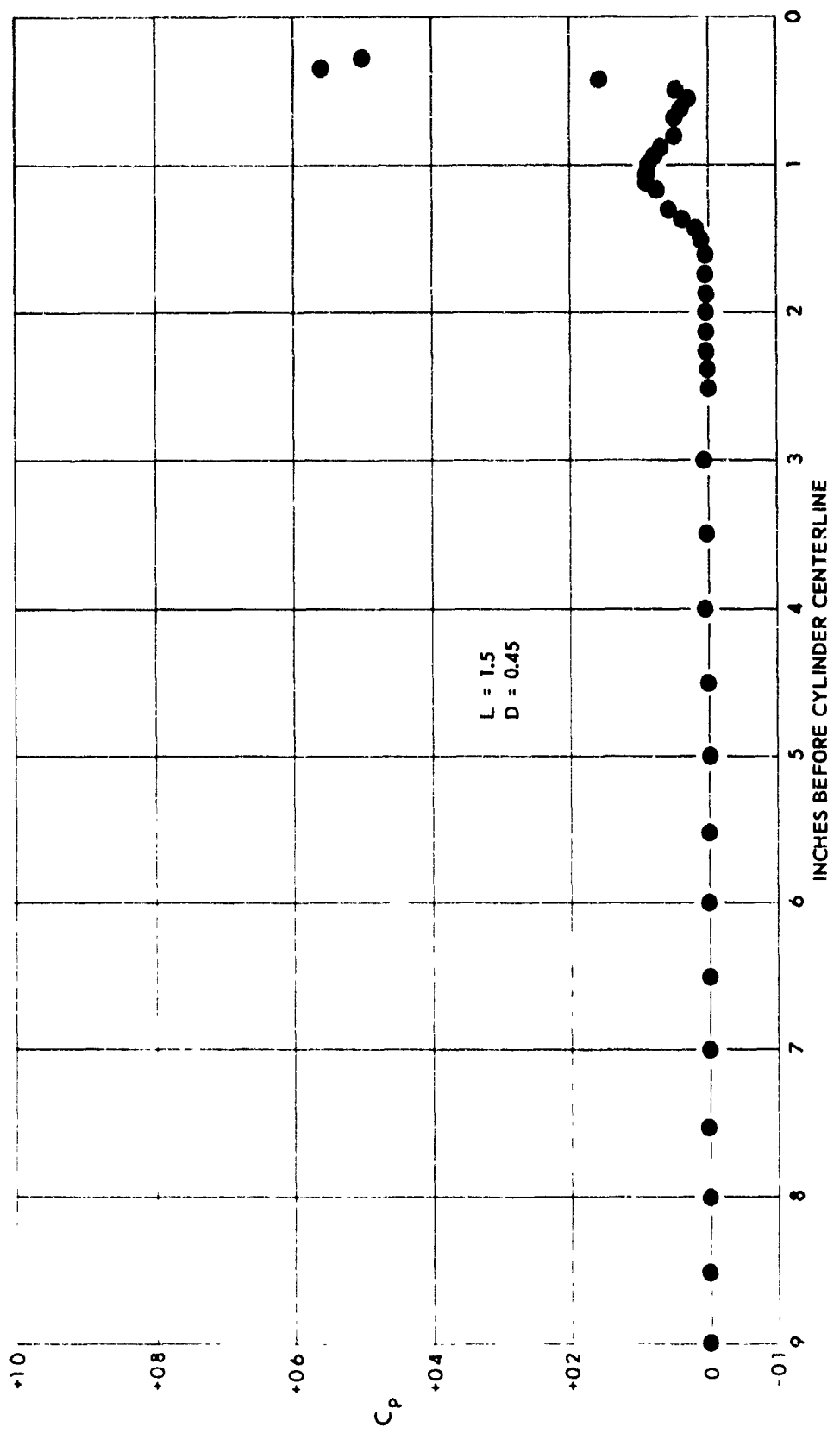


FIGURE 6c
 TYPICAL STATIC PRESSURE PROFILE

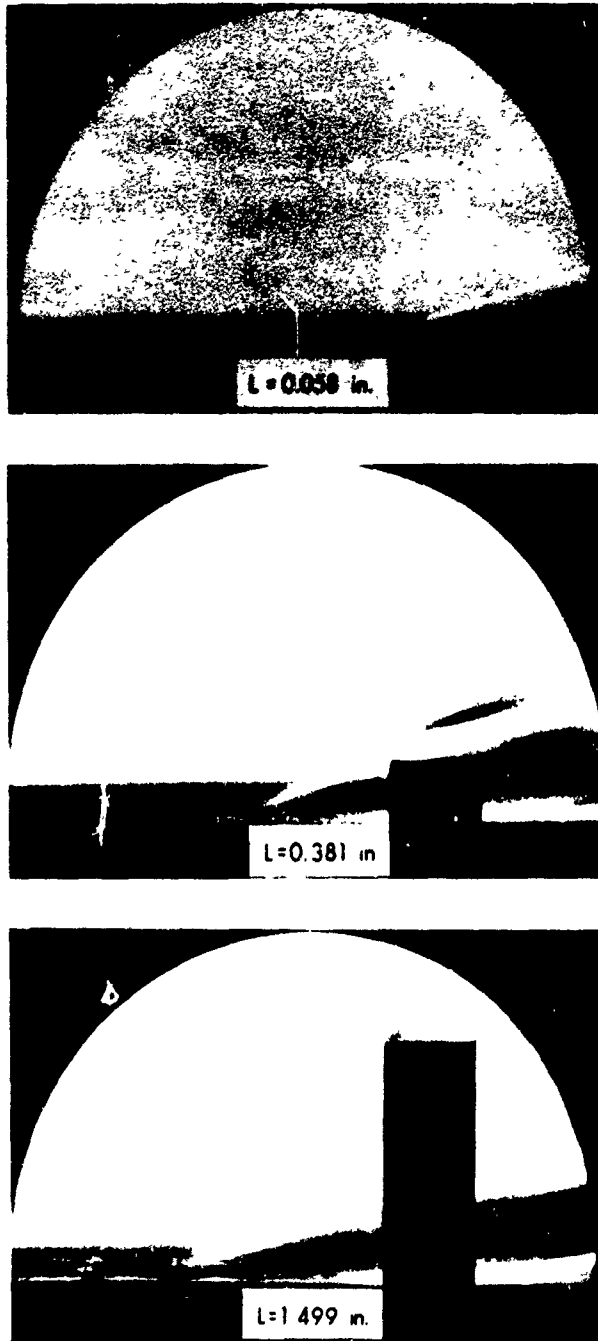


FIGURE 7
SCHLIEREN PHOTOGRAPHS OF SINGLE CYLINDERS
FROM REF. 1

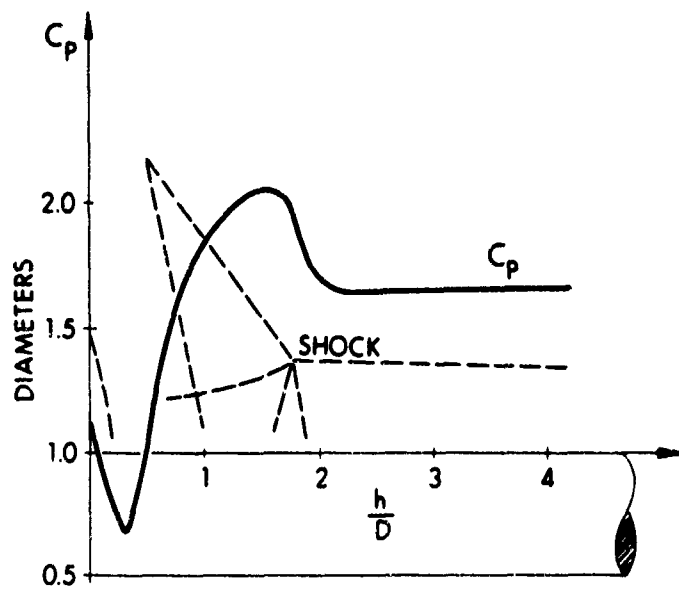


FIGURE 8
SHOCK SHAPE AND STAGNATION-LINE
PRESSURE DISTRIBUTION FROM Ref. 6

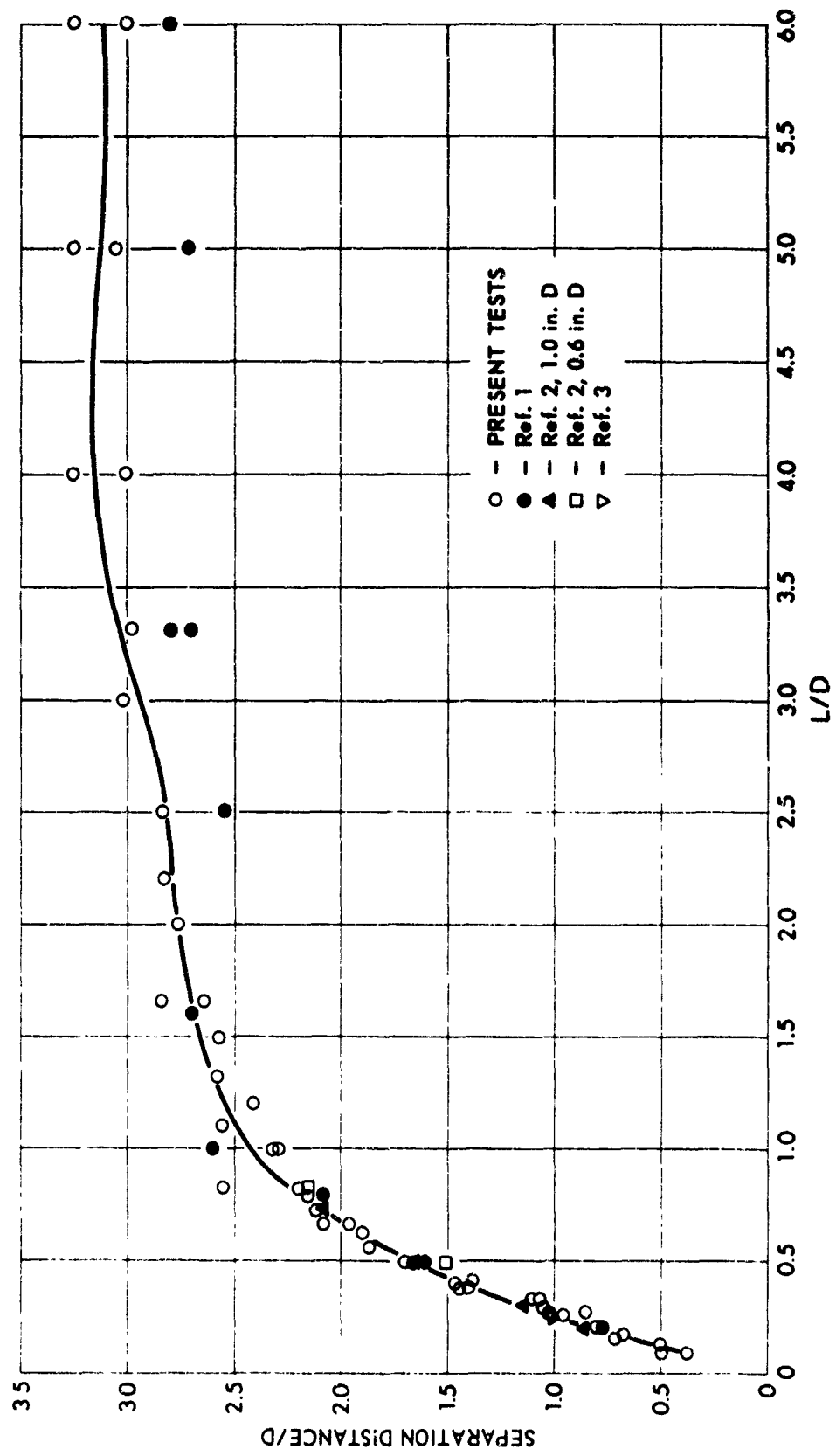


FIGURE 9
SEPARATION DISTANCE CORRELATION

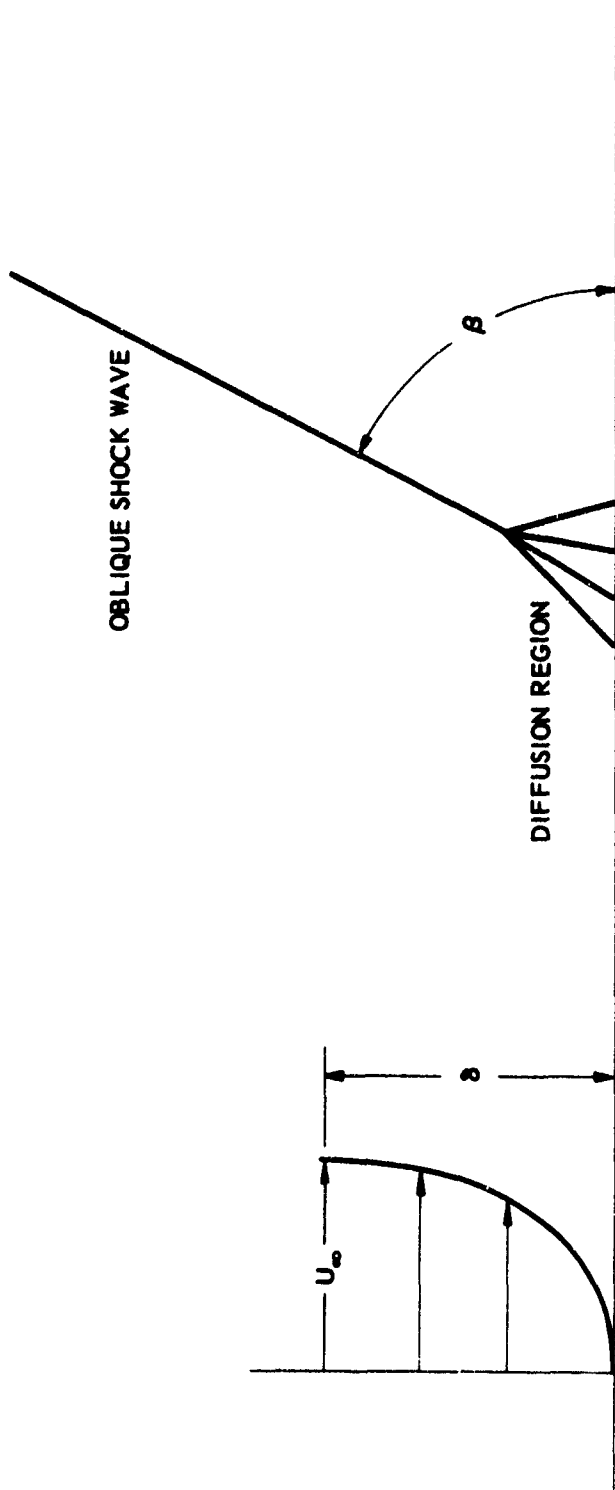


FIGURE 10
OBLIQUE SHOCK DIFFUSION
IN BOUNDARY LAYER FROM Ref. 5

UNCLASSIFIED

Security Classification

DOCUMENT CONTROL DATA - R & D		
<i>(Security classification of title, body of abstract and indexing annotation must be entered when the overall report is classified)</i>		
1. ORIGINATING ACTIVITY (Corporate author) Applied Research Laboratories The University of Texas at Austin Austin, Texas 78712		2a. REPORT SECURITY CLASSIFICATION UNCLASSIFIED
		2b. GROUP ---
3. REPORT TITLE TURBULENT BOUNDARY LAYER SEPARATION AHEAD OF CYLINDRICAL PROTUBERANCES IN SUPERSONIC FLOW		
4. DESCRIPTIVE NOTES (Type of report and inclusive dates) -----		
5. AUTHOR(S) (First name, middle initial, last name) James Harvel Mashburn		
6. REPORT DATE August 1969	7a. TOTAL NO. OF PAGES 59	7b. NO. OF REFS 11
8a. CONTRACT OR GRANT NO. APL/JHU Subcontract 271734, Task B	8b. ORIGINATOR'S REPORT NUMBER(S) ARL-TR-69-17	
b. PROJECT NO. c. d.	9b. OTHER REPORT NO(S) (Any other numbers that may be assigned this report) ---	
10. DISTRIBUTION STATEMENT This document has been approved for public release and sale; its distribution is unlimited.		
11. SUPPLEMENTARY NOTES -----	12. SPONSORING MILITARY ACTIVITY Naval Air Systems Command Department of the Navy Washington, D. C. 20360	
13. ABSTRACT The results of an experimental study of separation distances ahead of right circular cylinders mounted perpendicular to a flat plate are presented. The tests were conducted in a supersonic wind tunnel at a nominal test Mach Number of 4.8. Turbulent boundary layer conditions existed at the cylinder mounting position. All tests were for single cylinder configurations. The cylinders tested ranged in length from 1/16 in. to 1 1/2 in. and in diameter from 3/16 in. to 1 1/2 in. Experimental data were used to determine an empirical correlation between boundary layer separation distance and cylinder length. Comparison of results with other data sources showed the correlation in close agreement with previously observed boundary layer separation phenomena. (U)		

UNCLASSIFIED

Security Classification

14 KEY WORDS	LINK A		LINK B		LINK C	
	ROLE	WT	ROLE	WT	ROLE	WT
Supersonic drag Protuberance drag Cylindrical drag Drag prediction Direct drag measurement Separation						

DD FORM 1473 (BACK)
NOV 68
(PAGE 2)

UNCLASSIFIED

Security Classification